DEEPOLE QUASAR–A Physics-Informed Deep Convolutional Neural Network to Disentangle MRI Phase Contrast Mechanisms

Thomas Jochmann [1], Jens Haueisen [1], Robert Zivadinov [2,3] and Ferdinand Schweser [2,3]

[1] Technische Universität Ilmenau, Ilmenau, Germany; [2] Center for Biomedical Imaging at the Clinical and Translational Science Institute, University at Buffalo, The State University of New York
[3] Buffalo Neuroimaging Analysis Center, Department of Neurology; Jacobs School of Medicine and Biomedical Sciences at the University at Buffalo, The State University of New York

Summary

- Magnetic susceptibility is a physical property of brain tissues that changes with iron level and (de-)myelination.
- Mapping the susceptibility can help us improve our understanding of the brain and its diseases, such as Multiple Sclerosis and Alzheimer's Disease.
- ***Quantitative Susceptibility Mapping (QSM)*** derives the susceptibility using MRI. ***QUASAR*** adds a more sophisticated physical model to QSM. ***DEEPOLE-QUASAR*** is a deep learning approach to solve the QUASAR inverse problem.
- DEEPOLE-QUASAR separates the magnetic field into two components from different contrast mechanisms, yields an improved QSM map, and shows where in the brain the tissue does not adhere to the basic QSM model, e.g. where it is anisotropic.

Introduction

MAGNETIC SUSCEPTIBILITY IN THE BRAIN

- The tissue's magnetic susceptibility defines how strong the body perturbs the static magnetic field of an MRI.
- Thus, from measurements of the magnetic field's perturbation we can derive the magnetic susceptibility distribution. This is called *Quantitative Susceptibility Mapping (QSM)*.
- The magnetic susceptibility in the brain tissue is linked to iron and myelin. Therefore, researchers increasingly use QSM in clinical and pre-clinical studies.

QUANTITATIVE SUSCEPTIBILITY MAPPING (QSM)

- QSM requires the solution of the ill-posed inverse physical problem of the Larmor frequency distribution f:

$$f = d * \chi,$$

  where * denotes the 3D convolution, d is the unit dipole with Lorentzian sphere correction and χ is the magnetic susceptibility.
- The physical model of QSM neglects frequency contributions that are not directly related to isotropic magnetic susceptibility. QSM uses the *Lorentzian sphere approximation* which does not hold in anisotropic tissues, such as the brain [1].

QUANTITATIVE SUSCEPTIBILITY AND RESIDUAL MAPPING (QUASAR)

- Schweser and Zivadinov [2] have recently proposed an extended physical model for QSM, termed *QUASAR*.
- QUASAR aims to separate frequency contrast f_χ adhering to the Lorentzian sphere model and frequency contrast f_ρ that does not.
- QUASAR solves the highly underdetermined problem

$$f = f_\chi + f_\rho$$

  (with $f_\chi = d * \chi$) with respect to both χ and f_ρ.
- While QUASAR-QSM yields improved susceptibility maps, it is only partially able to disentangle f_ρ from f [2].

Here, we propose an approach to overcome this limitation of the original QUASAR algorithm by using **DEE**p learning of the **P**hase **O**rigin with a **L**orentzian sphere **E**stimation (**DEEPOLE**).

ISMRM Workshop on Machine Learning, Part II
October 25-28, 2018; Washington, D. C., USA

Corresponding author: F.S. (schweser@buffalo.edu)
Poster number: 18

Methods

3D U-NET: A DEEP CONVOLUTIONAL NEURAL NETWORK

We built a deep convolutional neural network (Python, Keras, Tensorflow) based on the U-Net architecture [3] and adapted to 3D input and 3D output fields with three-dimensional convolutions (Fig. 1).

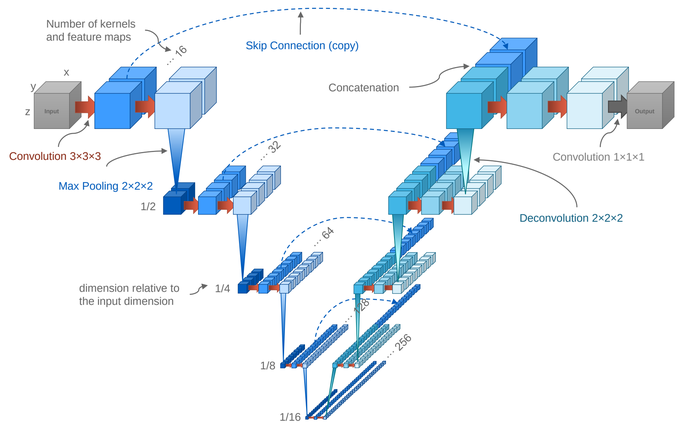

***Figure 1**. Architecture of the deep convolutional neural network for DEEPOLE. We adapted the 2D U-Net architecture [3] to 3D data.*

PHYSICS-INFORMED NETWORK TRAINING

- We trained the network to predict the volumetric scalar field f_ρ from the same-sized volumetric scalar field f (Fig. 2a).
- We generated models of χ and f_ρ (80×80×80 voxels) consisting of randomly sized, placed, and rotated boxes, ellipsoid shells, and lines (Fig. 2).
- We obtained f by computing the field perturbation f_χ via Fast Forward Field Computation [4] and adding it to the f_ρ model.
- The underdetermined nature of the problem requires incorporating domain knowledge into the training process. We restricted the data manifold by assuming that real-world χ and f_ρ share tissue boundaries, which was realized by using the same geometrical training structures but different intensities within the structures.
- The network was trained using 1000 pairs of f and f_ρ and was stopped when training and evaluation losses diverged.

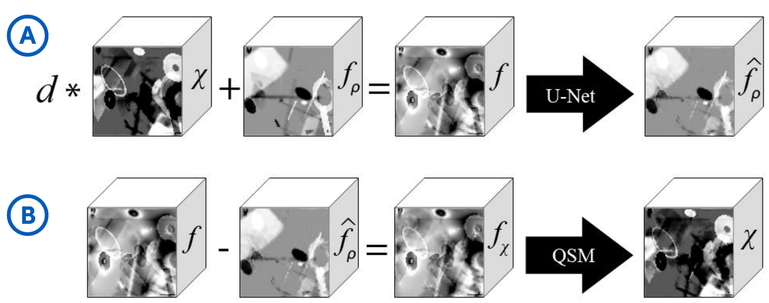

***Figure 2**. a) Training of the deep convolutional neural network (U-Net) to recover f_ρ from f using simulated Larmor frequency maps f obtained from source patterns of susceptibility χ and f_ρ. b) Subtracting the predicted f_ρ, $\hat{f}_\rho$, from f yields f_χ, which can be inverted to χ through QSM.*

EVALUATION

- To evaluate the algorithm *in vivo*, we used data acquired with an axial 3D multi-echo spoiled gradient recalled echo sequence (12 echoes; 3T).
- We calculated f_ρ with the proposed DEEPOLE QUASAR algorithm and, for comparison purposes, with the original QUASAR algorithm.
- For QSM, we subtracted the predicted f_ρ from the measured f and applied DeepQSM [5] (Fig. 2b).
- To evaluate the algorithm *in silico*, we assessed the difference between f_ρ predicted from simulated f and the ground truth.

Results

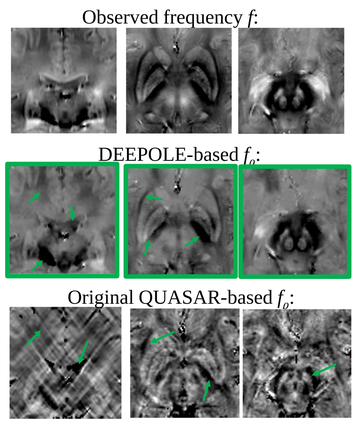

Figure 3 illustrates the application of DEEPOLE *in vivo* (middle) and compares the predicted f_ρ with the solution obtained with the original QUASAR algorithm (bottom). Both maps showed similar features (arrows) with the cerebrospinal fluid (CSF) appearing as hyper-intense compared to adjacent white matter (WM; arrows). Structures with high structural anisotropy were most hypo-intense (arrows: corticospinal tract, internal capsule, claustrum).
Original QUASAR-based maps presented f_ρ with a substantially higher artifact level than DEEPOLE-based maps.

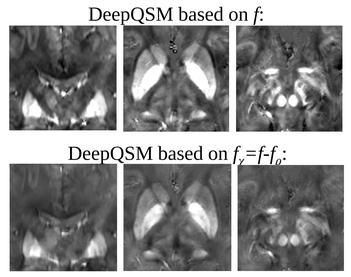

Figure 4 compares QSM using the observed frequency map ($f_\chi + f_\rho$; Fig. 3-top) with QSM using a frequency map obtained by correcting the observed map with the DEEPOLE-predicted map of f_ρ (Fig. 3-bottom and Fig. 2b).

The DEEPOLE susceptibility maps were less inhomogeneous in the WM compared to the conventional susceptibility maps (see corpus callosum) and showed lower susceptibility values in the gray matter. The *in silico* results were inconsistent showing highly accurate prediction in some cases and only partial source separation in others.

The computation time for the DEEPOLE prediction of f_χ and f_ρ from f was below 100 ms on an NVIDIA GeForce GTX 1080 GPU.

Discussion

- Our results illustrate the ability of deep neural networks to solve underdetermined source separation problems in MRI based on theory-guided learning from artificial training data.
- We expect that optimized network architectures and training data generation rules will further improve the source separation accuracy. A thorough validation of the method is needed, which needs to rely on both numerical simulations and histological experiments.
- Despite its limitations, the presented implementation improved the QSM reconstruction quality and provided frequency contrast related to mechanisms not accessible until recently and not accounted for in the established QSM model.
- Being primarily related to myelin and proteins in the WM, the f_ρ-contrast bears the potential of a unique and highly sensitive assessment of myelin-related pathology. Our method successfully separated this residual field component from the Lorentzian-sphere dipole component.

Conclusion

- Physics-informed deep convolutional neural networks are a promising tool for solving underdetermined source separation problems with a flexible incorporation of complex domain knowledge.
- The proposed approach sets the foundation for the quantification of biophysical tissue properties with MRI based on known physical interactions between tissue constituents, architecture and the MRI signal.

References

1. He & Yablonskiy, PNAS, 2009
2. Schweser & Zivadinov, NMR Biomed 2018
3. Ronneberer et al. ArXiv, 2015
4. Marques & Bowtell, Concept MRM B, 2005
5. Rasmussen et al. BioRxiv, 2018

mbl.bnac.net